

# Temperature dependence of the optical birefringence of $\text{MnF}_2$ , $\text{MgF}_2$ , and $\text{ZnF}_2$

D. P. Belanger,\* A. R. King, and V. Jaccarino

*Department of Physics, University of California, Santa Barbara, California 93106*

(Received 13 October 1983)

Measurements have been made of the temperature derivative of the optical birefringence  $d(\Delta n)/dT$  of (magnetic)  $\text{MnF}_2$  and the isostructural (nonmagnetic)  $\text{MgF}_2$  and  $\text{ZnF}_2$ . We show that the lattice contribution to  $d(\Delta n)/dT$  is *not* proportional to the anisotropy in the thermal expansion as had been previously conjectured. Instead, using a suitably weighted Debye plus Einstein phonon densities of states, a very good fit of the measured  $d(\Delta n)/dT$  to harmonic excitations of the lattice can be made for  $\text{MgF}_2$  and  $\text{ZnF}_2$  from  $5 \leq T \leq 300$  K. For  $T \ll \Theta_D$ ,  $d(\Delta n)/dT$  scales with  $\Theta_D$  as does the lattice specific heat  $C_L$ . By using this scaling property, the small lattice contribution to  $d(\Delta n)/dT$   $\text{MnF}_2$  may be deduced. The remaining, much larger, magnetic contribution can then be compared with the magnetic specific heat  $C_m$  over the range  $5 \text{ K} \leq T \leq 100 \text{ K}$ . The agreement found between the two is excellent. This definitive result establishes that the proportionality between  $C_m$  and the magnetic part of  $d(\Delta n)/dT$  extends well outside the critical region.

## I. INTRODUCTION

For more than a decade, optical linear magnetic birefringence ( $\Delta n$ ) has been used to study the magnetism of insulators. Ferrimagnets were the earliest systems investigated,<sup>1</sup> but it was later shown in the pioneering work of Jahn and Dachs<sup>2,3</sup> and Borovik-Romanov *et al.*<sup>4</sup> that  $d(\Delta n)/dT$  could be used to study the magnetic heat capacity  $C_m$  of anisotropic antiferromagnets (AF) both above and below  $T_N$ . In the intervening years, an increasing use has been made of the  $\Delta n$  technique in the study of pure AF systems of different space dimensionalities,<sup>4-11</sup> randomly mixed,<sup>12</sup> or diluted ones,<sup>13</sup> and the effects of pressure and magnetic fields<sup>6,7,14,15</sup> on the properties of some of these same systems.

There are a number of reasons as to why the  $\Delta n$  technique has been so widely applied to AF systems: (1)  $\Delta n$  measurements of high precision are easily made, (2) the temperature dependence of the nonmagnetic (lattice) birefringence is much smaller, relative to the magnetic part, when compared to what is found in conventional specific heat measurements, and (3) a very small volume of the crystal may be sampled by a focused laser beam in the linear magnetic birefringence (LMB) measurement. This latter attribute is particularly important in studies of mixed or diluted AF systems, where a gradient of the concentration causes a rounding of the transition temperature, thereby limiting the range of reduced temperature  $t = (T - T_N)/T_N$  over which critical phenomena may be studied.

Although the lattice contribution to the temperature derivative of the birefringence  $d(\Delta n)/dT$  is small, it is not negligible; that is to say, precise comparisons of the magnetic specific heat, as measured by conventional techniques, with that deduced from birefringence measurements, cannot be had without some "corrections" being made for the nonmagnetic background. This is particularly important if the comparison extends over a wide range of temperature. Only one attempt has been made to

understand the lattice contribution to  $d(\Delta n)/dT$ , in a systematic study of the transition-metal difluorides  $\text{XF}_2$  (with  $X = \text{Mn, Fe, Co, and Zn}$ ) and  $\text{MgF}_2$ . In that work,<sup>3</sup> Jahn established what he believed was a proportionality between the temperature dependence of the anisotropy in the lattice expansion and the temperature derivative of the birefringence;  $d(\Delta n)/dT = K[\beta_c(T) - \beta_a(T)]$  where  $\beta_c$  and  $\beta_a$  are the linear coefficients of thermal expansion in the  $c$  and  $a$  directions. We will review this in more detail in Sec. III.

In the present work, we reexamine this problem, from both an experimental and theoretical point of view, using new measurements of  $d(\Delta n)/dT$  vs  $T$  in  $\text{MnF}_2$ ,  $\text{MgF}_2$ , and  $\text{ZnF}_2$ . We first show that  $d(\Delta n)/dT$  and  $\beta_c(T) - \beta_a(T)$  are *not* proportional to each other over a wide range of temperatures. Instead, we find that by using a suitably weighted Debye plus Einstein phonon density of states, an excellent fit of the measured  $d(\Delta n)/dT$  to the harmonic excitations of the lattice can be made for  $\text{MgF}_2$  and  $\text{ZnF}_2$  over the entire range of temperatures. Moreover,  $d(\Delta n)/dT$  scales as expected with  $\Theta_D$ . With this scaling established, the lattice contribution to  $d(\Delta n)/dT$  in  $\text{MnF}_2$  may be calculated and the remaining magnetic part compared with  $C_m$  over the range  $5 \leq T \leq 100$  K. The agreement found is most satisfactory.

## II. EXPERIMENTAL METHOD AND RESULTS

### A. Experimental method

The linear birefringence was measured using the Sénarmont technique with a photoelastic modulator for increased sensitivity. The optical arrangement is shown schematically in Fig. 1. A 2-mW He-Ne laser ( $\lambda = 632.8$  nm) with internal polarization is used to eliminate polarization fluctuations in the emitted light, which is then polarized at  $45^\circ$  relative to the sample's optical axis, by the first calcite crystal. The light emerges from the sample elliptically polarized, with one axis of the ellipse parallel to

the initial polarization direction. A mica  $\lambda/4$  plate retards the phase of  $E_{\parallel}$  relative to  $E_{\perp}$  by  $90^\circ$ , thereby changing the elliptically polarized to linearly polarized light. The angle  $\theta$  through which the initial polarization has rotated is equal to half of the relative phase shift  $\phi$  occurring in the sample;  $\theta = \phi/2 = \pi \Delta n t / \lambda$ , where  $\Delta n$  is the sample birefringence and  $t$  its thickness.

The analyzing calcite polarizer measures  $\theta$  by *minimizing* the intensity of the light incident on the photomultiplier detector. It is mounted in the hub of a carefully centered 72-tooth gear. This is driven by a worm gear, coupled to a stepper motor, with 48 steps per revolution, through an additional 10:1 gear reduction. There are 34560 steps per revolution of the analyzing polarizer. Backlash in the gears is less than one step of the stepper motor. This yields an angular resolution of  $\sim 0.01^\circ$  which, for a typical 4-mm sample, results in a resolution of approximately  $10^{-8}$  in the birefringence. The photoelastic modulator provides a small depth of modulation of  $\Delta n \equiv \delta \sin \omega t$ , at  $\omega = 2\pi \times 50$  KHz, which permits use of lock-in null detection. For small deviations  $\gamma$  of the analyzing polarizer from null, the transmitted light intensity

$$I \propto (\delta^2/8)(1 - \sin 2\omega t) - \gamma \delta \sin \omega t.$$

The lock-in amplifier is set to detect the in-phase component at frequency  $\omega$  and hence gives an output proportional to  $\gamma$ . The effects of a small variation of  $\Delta n$  across the sampled region of the crystal being studied, of imperfect optical components or slight optical misalignment, or

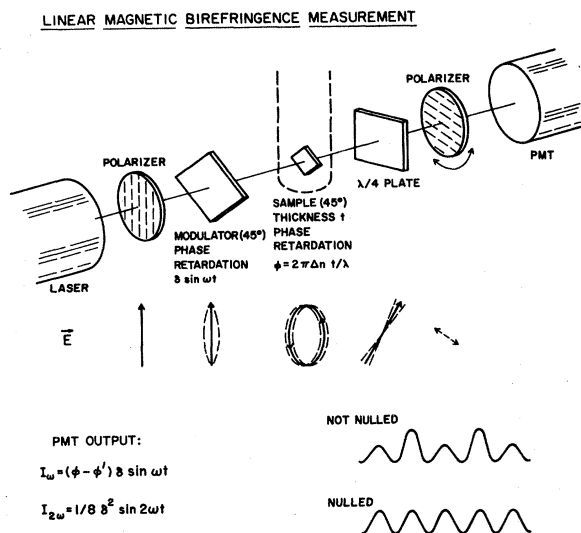


FIG. 1. Schematic representation of the Sénarmont compensator used for measuring  $d(\Delta n)/dT$ . Lock-in detection of the  $\omega = 50$  kHz component of the photomultiplier output (PMT) allows null detection. The sensitivity in  $\Delta n$  is  $10^{-8}$  for a typical sample.

of a small amount of linear dichroism in the sample, are only to decrease the quality of the null with a resultant increase in the output noise signal.

The cryostat was designed with a tail to fit in a 20-kG electromagnet; details of the tail and sample holder are shown in Fig. 2. The fused quartz windows on the outer wall are mounted in a strain-free manner and produce negligible residual birefringence. No windows are used on either the nitrogen or sample heat shields. The sample holder is supported by the 0.010-in.-thick stainless-steel wall of the heat exchanger, and the heat flow from the sample block to the liquid-helium reservoir is determined by the pressure of the He exchange gas. To provide good thermal contact with minimal strain, the sample was held in place with a light coating of Apiezon-*N* grease and the slight pressure of the Cu-Be spring.

A commercial carbon glass resistor was used as the primary thermometer both for its good sensitivity over the (1.5–300)-K temperature range and its relatively small sensitivity to magnetic fields. Thermal cycling effects, which occur when the carbon glass resistor is brought back to room temperature, limit the reproducibility of a repeated measurement at 70 K to about  $\pm 30$  mK; hence for critical phenomena studies, all measurements were made in a single run at low temperatures. Four-wire measurements were made at a low frequency (17 Hz), to take advantage of the higher sensitivity and accuracy of ac resistance measurements, using a current ratio generator<sup>16</sup>

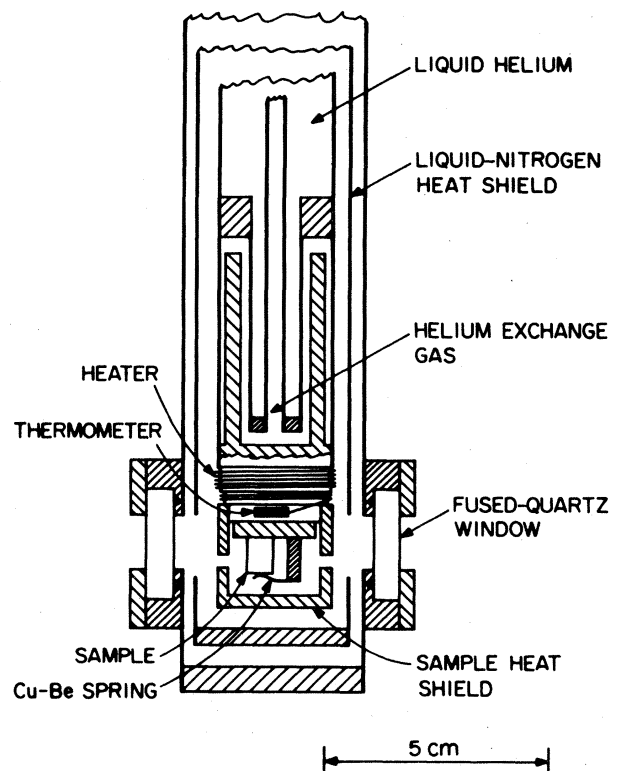


FIG. 2. Tail of the optical cryostat. Residual birefringence in the quartz windows is negligible. The temperature could be stabilized to  $100 \mu\text{K}$  at 70 K.

and lock-in null detection. Sample temperatures could be stabilized to within  $100 \mu\text{K}$  at 70 K. The absolute accuracy of the temperature measurement was  $\pm 0.1 \text{ K}$  at 70 K.

The  $\text{MnF}_2$ ,  $\text{MgF}_2$ , and  $\text{ZnF}_2$  crystals were grown in the University of California (Santa Barbara) Physics Department Materials Preparation Laboratory using a stationary solidification modification of the Bridgmann-Stockbarger method. Oriented samples cut from the boule were typically 4 mm thick. Optically flat faces were ground, first with a  $3\text{-}\mu\text{m}$ , then a  $1\text{-}\mu\text{m}$ , and finally a  $0.3\text{-}\mu\text{m}$  alumina power placed on cloth pads on glass. A special sample polishing holder was used so that the faces could be kept parallel to each other to within one part in 500, as determined from the coincidence of the back reflection of a laser beam from the two faces.

### B. Experimental results

The temperature derivative of the birefringence  $d(\Delta n)/dT$  vs  $T$  for  $\text{MgF}_2$ ,  $\text{ZnF}_2$ , and  $\text{MnF}_2$  are shown as the solid dots in Figs. 3, 4, and 5, respectively. The derivative was obtained by taking the difference between successive measurements at  $T_i$  and  $T_{i+1}$  and dividing by the interval of temperature  $\Delta T \equiv T_{i+1} - T_i$ ; this value of  $\Delta n/\Delta T$  was then plotted at the mean temperature  $(T_{i+1} + T_i)/2$ . Taking small intervals of temperature tends to increase the scatter in  $d(\Delta n)/dT$  vs  $T$  as compared with what is observed directly in  $\Delta n$  vs  $T$ . For the subsequent analysis to be given of the nonmagnetic contributions to  $d(\Delta n)/dT$ , the accuracy with which  $d(\Delta n)/dT$  vs  $T$  has been obtained is quite adequate.

The high precision of the data obtained in the present measurements are to be compared with the earlier work of Jahn.<sup>3</sup> For example, Jahn could detect no variation in  $d(\Delta n)/dT$  in  $\text{ZnF}_2$  below 70 K. Since the interpretation we will give to  $d(\Delta n)/dT$  vs  $T$  depends strongly upon fitting a phenomenological model to both the low- and high- $T$  behavior of  $d(\Delta n)/dT$ , it is not surprising that a

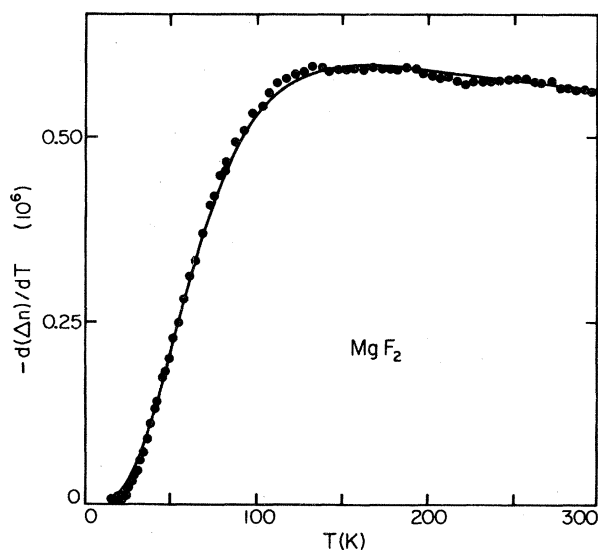


FIG. 3.  $d(\Delta n)/dT$  vs  $T$  for  $\text{MgF}_2$ . The solid curve is a fit using a Debye-type and an Einstein-type contribution.

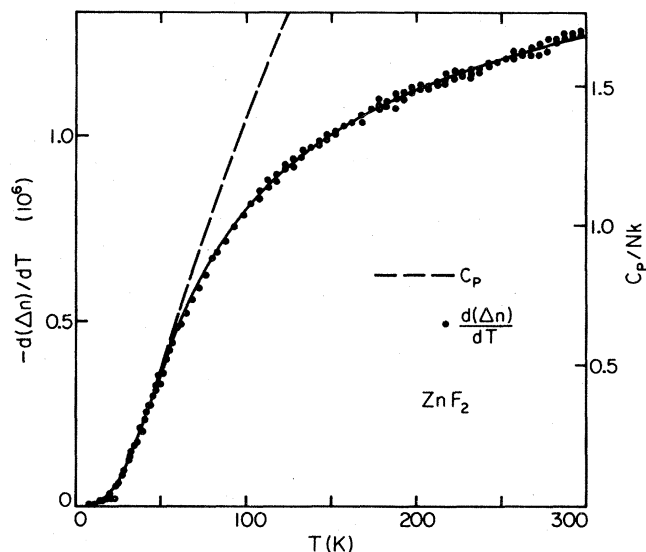


FIG. 4.  $d(\Delta n)/dT$  vs  $T$  for  $\text{ZnF}_2$ . The solid curve is a fit using  $C_p$  and an Einstein-type contribution.

more elaborate treatment of the problem can now be given than was possible with the earlier measurements.

## III. ANALYSIS AND INTERPRETATION OF $d(\Delta n)/dT$

### A. Nonmagnetic $\text{MgF}_2$ and $\text{ZnF}_2$

By definition, the optical birefringence is the anisotropy in the index of refraction ( $n$ ); for a uniaxial crystal  $\Delta n \equiv n_e - n_o$ , which means  $\Delta n$  can be positive or negative. Although formal theories exist for obtaining expressions for the optical dielectric constant  $\epsilon(\omega)$  in ionic crystals, and hence  $n$  ( $n^2 = \epsilon$ ), they are confined to calculations of

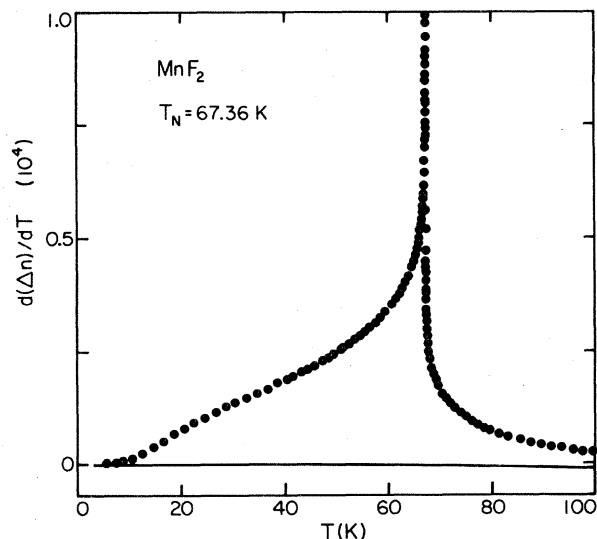


FIG. 5.  $d(\Delta n)/dT$  vs  $T$  for  $\text{MnF}_2$ . The solid curve is the estimated lattice contribution which is negative and very small with respect to the magnetic part.

the magnitude of  $n$  and still cruder estimates of  $\Delta n$  at  $T=0$  K. No attempt has been made, to our knowledge, to obtain the temperature dependence of  $d(\Delta n)/dT$  from first principles. Hence one must let experiment be the guide in suggesting a phenomenological model for explaining the observed behavior of  $d(\Delta n)/dT$  vs  $T$ .

It was evident to Jahn<sup>3</sup> that the shape of his  $\Delta n$ -vs- $T$  curves qualitatively resembled the corresponding ones for the lattice vibrational energy,  $U_L$  vs  $T$ . However, in the absence of high-precision measurements of  $d(\Delta n)/dT$  at low  $T$ , he elected to identify the variation of  $d(\Delta n)/dT$  with lattice anharmonicity by comparing the anisotropy in the thermal expansion  $\beta_c(T) - \beta_a(T)$  with  $d(\Delta n)/dT$  at higher temperatures. Within the accuracy of his measurements, and those of  $\beta_c(T) - \beta_a(T)$ , he showed that

$$\kappa \equiv \left[ \frac{d(\Delta n)}{dT} \right] / [\beta_c(T) - \beta_a(T)] \quad (1)$$

is approximately constant above 200–300 K for nearly all of the transition-metal difluorides but that  $\kappa$  varied considerably both below these temperatures and from compound to compound. The latter property he identified with the differing degrees of covalency associated with the  $X^{2+} - F^-$  bond.

We tested the above relation, Eq. (1), by comparing  $d(\Delta n)/dT$  vs  $T$  with accurate measurements of  $\beta_c(T) - \beta_a(T)$  for  $\text{MgF}_2$ ,<sup>17</sup> in the range  $0 < T < 300$  K. As seen

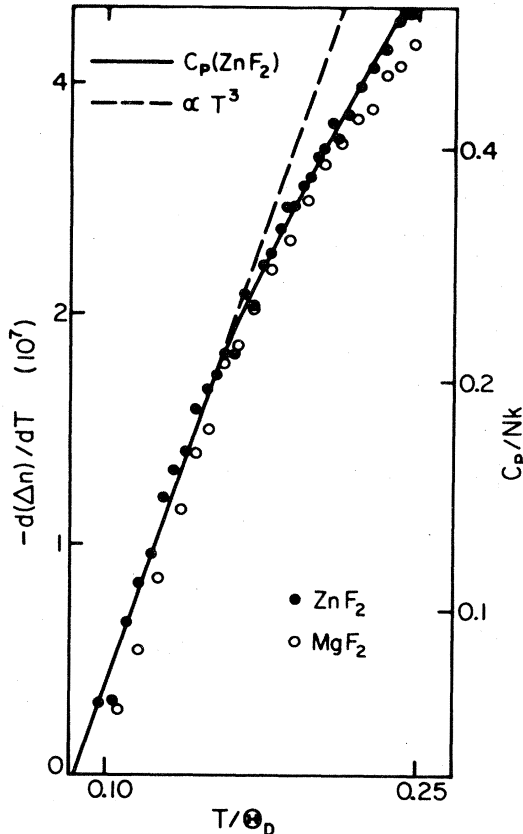


FIG. 6.  $\log d(\Delta n)/dT$  vs  $\log T/\Theta_D$  for  $\text{MgF}_2$  and  $\text{ZnF}_2$  and  $\log C_p/Nk$  vs  $\log T/\Theta_D$  for  $\text{ZnF}_2$ .

in Fig. 3,  $-d(\Delta n)/dT$  has a broad maximum in the neighborhood of 150 K, whereas the anisotropy in the thermal expansion monotonically increases with  $T$ . Additional evidence against such a simple proportionality comes from piezo-optic, uniaxial compression ( $p$ ) experiments on  $\text{MnF}_2$  (Ref. 18) and  $\text{MgF}_2$  (Ref. 19) at ambient temperatures. Measurements of  $d(\Delta n)/dp$  parallel and perpendicular to the  $c$  axis have been made on both crystals. Using the known elastic constants<sup>20,21</sup> to obtain the anisotropy in the compressibility, one finds that the proportionality between  $d(\ln a)/dT - d(\ln c)/dT$  and  $d(\Delta n)/dT$ , although comparable in magnitude to the proportionality between  $d(\ln a)/dp - d(\ln c)/dp$  and  $d(\Delta n)/dp$ , is *opposite in sign*. We further note that such a treatment neglects one degree of freedom of the lattice, namely, the  $u$  parameter which specifies the position of the fluorine ions. Although accurate measurements of  $du/dT$  have not been made, it has been shown that  $\Delta n$  may vary strongly with  $u$ .<sup>22</sup> For these several reasons there appears to be little merit in pursuing the approach further; i.e., correlating  $d(\Delta n)/dT$  directly with lattice anharmonicity.

Instead, we note that the low-temperature behavior of  $d(\Delta n)/dT$  vs  $T$  for both  $\text{MgF}_2$  and  $\text{ZnF}_2$  closely follows a  $(T/\Theta_D)^3$  law, as does the lattice specific heat  $C_L$ , in the region  $T \ll \Theta_D$ , the Debye temperature, as is shown in Fig. 6. This suggests that one might try to relate the variation of  $\Delta n$  with  $T$  to the lattice vibrational energy  $U$  with  $T$ ; this is to say, we associate the changes in  $\Delta n$  with  $T$  directly with the *harmonic* excitations of the lattice.

As the simplest possible model, we approximate the specific heat  $C_L$  and  $d(\Delta n)/dT$  by a combination of a Debye and Einstein functions but we allow the factors weighting the contributions of the two functions to  $d(\Delta n)/dT$  to be different from those which are the prescribed weighting in the case of  $C_L$ . This may be viewed as allowing for a different amplitude (and possible sign) for the optical-phonon contribution, to  $d(\Delta n)/dT$  as compared with that produced by excitation of the acoustic phonons. As is clearly apparent from Fig. 7, the phonon dispersion curves for these materials are extremely complex. This approach is admittedly simplistic insofar as it assumes the contributions to  $d(\Delta n)/dT$  of *all* acoustic phonons may be represented by a *single* effective acoustic mode, and likewise in regards to *all* optical phonons. It follows then that

$$C_L/Nk = D(x_D) + 2E(z_E) \quad (2)$$

and

$$\frac{-d(\Delta n)}{dT} = AD(x_D) + BE(z_E). \quad (3)$$

The Debye and Einstein functions are defined by

$$D(x_D) = 3x_D^{-3} \int_0^{x_D} x^4 e^x / (e^x - 1)^2 dx \quad (4)$$

and

$$E(z_E) = [\exp(z_E) - 1]^{-2} z_E^2 \exp z_E, \quad (5)$$

respectively, with  $x_D \equiv \Theta_D/T$  and  $z_E \equiv \Theta_E/T$ . A fit of the measured  $C_L$  vs  $T$  for  $\text{MgF}_2$  has given  $\Theta_D = 318$  K

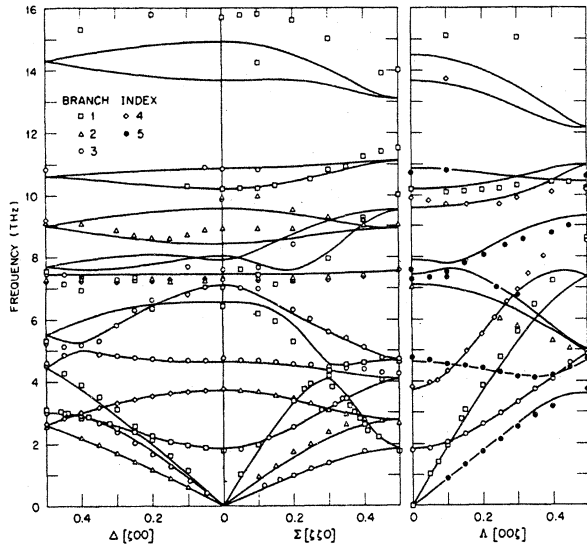


FIG. 7. Acoustical and optical phonon dispersion ( $\omega$  vs  $\vec{k}$ ) in  $\text{MnF}_2$ ; the solid lines are calculated using a simple shell model (Ref. 31). The dispersion for  $\text{MgF}_2$  is qualitatively similar (Ref. 32).

(Ref. 17) and  $\Theta_E = 553$  K.<sup>23</sup> Using these values for  $\Theta_D$  and  $\Theta_E$ , the fit of  $d(\Delta n)/dT$  vs  $T$  to Eq. (3) shown in Fig. 3 yields values of  $A = 9.2 \times 10^{-7}$  and  $B = 4.0 \times 10^{-7}$ ; the units of  $A$  and  $B$  are  $\text{K}^{-1}$ .

If the same procedure is repeated for  $\text{ZnF}_2$ , a good fit is obtained for  $A = 8.4 \times 10^{-7}$  and  $B = 5.6 \times 10^{-7}$ , using the values  $\Theta_D = 250$  K and  $\Theta_E = 456$  K previously obtained from x-ray studies.<sup>24</sup> However, a much better fit may be made using the measured  $C_L$ , since the latter is not that well represented by the Debye approximation at the temperatures of interest here. To accomplish this we used the empirical relation

$$\frac{-d(\Delta n)}{dT} = A' \frac{C_L}{Nk} + B'E(z) \quad (6)$$

and obtained the fit shown in Fig. 4 with the values  $A' = 8.4 \times 10^{-7}$  and  $B' = 11.2 \times 10^{-7}$ . Since  $C_L/Nk \simeq D(x_D) + 2E(z_E)$ , it follows that  $A = A'$  and  $B = 2A' + B'$ . The point to be made here is that the strict proportionality between  $d(\Delta n)/dT$  and  $C_L$  at low  $T$  transcends the questionable validity of the Debye approximation to  $C_L$  in this temperature region.

Although results have been obtained on only two nonmagnetic  $\text{XF}_2$  compounds with the rutile structure, the fact that the amplitude of  $d(\Delta n)/dT$  scales with  $T/\Theta_D$  at low  $T$ , as demonstrated in Fig. 6, suggests a procedure for estimating the lattice (background) contribution to  $d(\Delta n)/dT$  in the isomorphous antiferromagnet  $\text{MnF}_2$ . First, assuming that the low- $T$  nonmagnetic contribution scales as  $T/\Theta_D$ , we take the measured  $C_L/Nk$  for  $\text{ZnF}_2$ , rescaled for the small difference in  $\Theta_D$  [ $\Theta_D = 236$  K for  $\text{MnF}_2$  (Ref. 24)], and the value  $A' = 8.4 \times 10^{-7}$ , to construct the low-temperature lattice contribution to  $d(\Delta n)/dT$  using Eq. (6). To fit the Einstein-type contribution, with  $\Theta_E = 413$  K (Ref. 24), we have measured  $d(\Delta n)/dT$  in  $\text{MnF}_2$  for  $T$  up to 550 K ( $\sim 8.3T_N$ ), at

which point the magnetic part  $[d(\Delta n)/dT]_m$  is negligible. A fit to the high- $T$  data, shown in Fig. 8, yields the value  $B' = -5.4 \times 10^{-7}$ . Figure 5 shows the constructed lattice contribution  $[d(\Delta n)/dT]_L$  below 100 K.

The first point to be noted is that the relative nonmagnetic contribution to the measured  $d(\Delta n)/dT$  is extremely small below 200 K, and any moderately accurate procedure used to correct for it would certainly make possible a rather precise determination of  $[d(\Delta n)/dT]_m$ . Secondly, the ratio  $[d(\Delta n)/dT]_L/[d(\Delta n)/dT]_m$  is much smaller than the corresponding ratio  $C_L/C_m$  of lattice to magnetic contributions to the total specific heat; thus we expect the separation of lattice and magnetic contributions can be made more accurately for  $d(\Delta n)/dT$  than for the measured specific heat. However, if we assume  $C_m$  can be accurately separated from  $C_L$ , as was done by Boo and Stout,<sup>25</sup> then we are in a position to test whether the magnetic part of the birefringence  $[d(\Delta n)/dT]_m$  is proportional to  $C_m$ , i.e.,

$$\frac{C_m}{Nk} = \tilde{K} \left[ \frac{d(\Delta n)}{dT} \right]_m \quad (7)$$

If the proportionality in Eq. (7) holds,  $\tilde{K}$  may be determined without regard to the measurements of  $C_p$ . Since the total magnetic entropy  $S_m = Nk \ln(2S + 1)$ , it follows from Eq. (7) that, with  $S = \frac{5}{2}$ ,

$$\ln 6 = \tilde{K} \int_0^\infty dT T^{-1} \frac{d(\Delta n)}{dT} \quad (8)$$

With the entropy to be gained above 550 K being less than  $10^{-3}$  of the total, as estimated from high-temperature expansions,<sup>26</sup> it is accurate to replace the upper limit by  $T = 550$  K in Eq. (8); then numerically integrating the data shown in Figs. 5 and 8 we obtain  $\tilde{K} = 5.68 \times 10^{-4}$  K. If the nonmagnetic part had not been subtracted before integrating over this temperature range, the calculated  $\tilde{K}$  would have been only 6% smaller. We therefore believe the procedure used to determine  $\tilde{K}$  must be accurate to about 1%.

We may now directly test Eq. (7) by taking the ratio of  $C_m$ , as determined from  $C_p$ , to  $C_m = Nk\tilde{K}[d(\Delta n)/dT]_m$  and plotting it versus  $T$ . This is shown in Fig. 9 for the range  $10 \leq T \leq 100$  K. Remarkable agreement is found in that the ratio is scattered within  $\pm 5\%$  of unity, which is within the error for the determination of  $C_m$  directly from  $C_p$  in this temperature range; the corresponding uncertainties in  $[d(\Delta n)/dT]_m$  are considerably less. The agreement confirms that the correction of  $d(\Delta n)/dT$  for the nonmagnetic lattice contribution and the normalization of  $[d(\Delta n)/dT]_m$  to the magnetic entropy are most adequate.

A completely independent test of Eq. (7) and determination of  $\tilde{K}$  may be had from a study of the critical behavior of  $C_p$  and  $\Delta n$  in region very close to  $T_N$ . It is well known<sup>27</sup> that, for small values of  $|t| = |(T - T_N)/T_N|$ ,  $C_p$  may be fit to the expression

$$\frac{C_p}{Nk} = (A/\alpha) |t|^{-\alpha} + B + Et \quad (9)$$

for  $t > 0$  and with amplitude  $A'$  for  $t < 0$ . The  $B + Et$  terms are an adequate representation of the slowly vary-

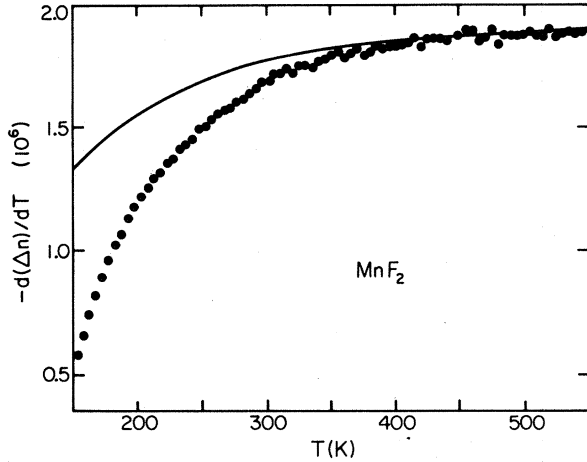


FIG. 8.  $d(\Delta n)/dT$  vs  $T$  for  $\text{MnF}_2$  at high temperatures. The solid curve is an estimate of the lattice contribution.

ing, nonsingular magnetic and *large* nonmagnetic lattice contributions. Likewise, the birefringence results may be expressed as

$$\frac{d(\Delta n)}{dT} = (\tilde{A}/\alpha) |t|^{-\alpha} + \tilde{B} + \tilde{E}t \quad (10)$$

for  $t > 0$  and with amplitude  $\tilde{A}'$  for  $t < 0$ . The  $\tilde{B} + \tilde{E}t$  terms are an adequate representation of the slowly varying nonsingular magnetic and *small* nonmagnetic lattice contributions. Note that the  $B + Et$  terms in Eq. (9) are *not* related to the  $\tilde{B} + \tilde{E}t$  terms in Eq. (10) by the same factor  $\tilde{K}$  that we postulate for the ratios  $A/\tilde{A}$  and  $A'/\tilde{A}'$ , a point to which we will return.

In the analysis of the birefringence data it is more convenient to use the results for  $\Delta n$  vs  $T$  directly and hence the temperature integral of Eq. (10) was first obtained. Since our main purpose is to compare  $A$  and  $\tilde{A}$ , we have fixed the parameters  $\alpha = 0.11$  (Ref. 28) and  $A/A' = \tilde{A}/\tilde{A}' = 0.53$  (Ref. 5) to their known three-dimensional Ising values. The values obtained for the amplitudes and "background" constants from the separate fits of the  $C_L$  and  $\Delta n$  are collected in Table I. The proportionality constant  $\tilde{K} = A/\tilde{A} = (5.51 \pm 0.03) \times 10^{-4}$  K differs by 3% from the value  $\tilde{K} = 5.68 \times 10^{-4}$  K obtained independently from the entropy normalization considerations. The errors quoted for the critical parameters are standard errors obtained from the nonlinear least-

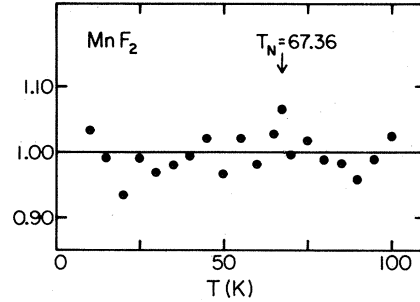


FIG. 9. Ratio of  $C_m$  determined solely from  $\Delta n$  data to  $C_m$  determined from  $C_p$  data for  $5 \leq T \leq 100$  K for  $\text{MnF}_2$ .

squares-fitting routine. They reflect neither the systematic errors in the measurements nor deviations of the data from pure Ising behavior.  $\text{MnF}_2$  exhibits pronounced Ising-to-Heisenberg crossover effects within the critical region. Even for  $|t| \ll 10^{-2}$ , for which the crossover effects are less important, larger systematic errors are evident for  $\text{MnF}_2$  than for the more Ising-like isomorphous antiferromagnet  $\text{FeF}_2$ .<sup>5</sup> Hence, we consider the value of  $\tilde{K}$  determined from the critical behavior to agree quite well, within experimental uncertainty, with the value of  $\tilde{K}$  derived from the entropy arguments presented earlier.

With the gratifying agreement in the value of the proportionality constant  $\tilde{K}$  obtained from the two independent methods, we should also expect consistency between the values of  $B$  and  $E$  and those of  $\tilde{B}$  and  $\tilde{E}$ . The nonsingular magnetic contributions to these terms are simply related by  $\tilde{K}$ . The lattice contributions are not related, but they have been determined for  $C_L$  and Boo and Stout<sup>25</sup> and for  $d(\Delta n)/dT$  using Eq. (6), as previously described. In Table II are shown the values of  $B$ ,  $E$ ,  $\tilde{B}$ , and  $\tilde{E}$  obtained from the critical region fits of the data. Also shown are the calculated lattice contributions for each parameter and the magnetic contributions which are simply obtained by subtraction. While the magnetic parts of  $B$  and  $\tilde{B}$  agree quite well, those of  $E$  and  $\tilde{E}$  differ somewhat. However, for the small range of reduced temperature ( $10^{-4} \leq |t| \leq 5 \times 10^{-3}$ ) used in the fitting, we do expect the terms  $Et$  and  $\tilde{E}t$  to be most susceptible to systematic errors, and deviations from the true value of the order of two standard deviations are not serious. We have, then, complete consistency in the determination of the magnetic and nonmagnetic parts of  $C$  and  $d(\Delta n)/dT$  in the critical

TABLE I. Parameters obtained from fits of the  $\Delta n$  and  $C_p$  data to Eqs. (10) and (9), respectively, for reduced temperatures  $10^{-4} \leq |t| \leq 5 \times 10^{-3}$ .

	$\frac{C_p}{Nk}$		$\Delta n$
$T_N$	$67.270 \pm 0.002$	$T_N$	$67.360 \pm 0.001$
$\alpha$	$0.11^a$	$\alpha$	$0.11^a$
$A/A'$	$0.53^a$	$\tilde{A}/\tilde{A}'$	$0.53^a$
$A'$	$0.245 \pm 0.001$	$\tilde{A}^{-1}$ ( $\text{K}^{-1}$ )	$(4.45 \pm 0.01) \times 10^{-6}$
$B$	$1.83 \pm 0.01$	$\tilde{B}$ ( $\text{K}^{-1}$ )	$-(1.13 \pm 0.01) \times 10^{-5}$
$E$	$5.26 \pm 0.51$	$\tilde{E}$ ( $\text{K}^{-1}$ )	$-(4.22 \pm 1.94) \times 10^{-5}$

<sup>a</sup>Fixed to  $d=3$  Ising values.

TABLE II. Magnetic and nonmagnetic contributions to the nonsingular terms of Eqs. (9) and (10).

	Total	Nonmagnetic	Magnetic	Normalized magnetic $\bar{K} = 5.51 \times 10^4 \text{ K}$
$B$	$1.83 \pm 0.01$	$2.43 \pm 0.12^a$	$-0.60 \pm 0.13$	$-0.60 \pm 0.13$
$\tilde{B}$	$-(1.13 \pm 0.01) \times 10^{-5}/\text{K}$	$-0.06 \times 10^{-5}/\text{K}$	$-(1.07 \pm 0.01) \times 10^{-5}/\text{K}$	$-0.59 \pm 0.01$
$E$	$5.26 \pm 0.51$	$3.57 \pm 0.36^a$	$1.7 \pm 0.9$	$1.7 \pm 0.9$
$\tilde{E}$	$-(4.22 \pm 1.94) \times 10^{-5}/\text{K}$	$-0.008 \times 10^{-5}/\text{K}$	$-(4.1 \pm 1.9) \times 10^{-5}/\text{K}$	$-2.3 \pm 1.1$

<sup>a</sup>Assuming an accuracy of 5% and 10% in the determination of the non-magnetic parts of  $B$  and  $E$ , respectively.

region and over the large temperature range  $5 \leq T \leq 100$  K.

#### IV. SUMMARY AND DISCUSSION

Two mechanisms have been identified<sup>29,30</sup> as contributing to the magnetic part of  $d(\Delta n)/dT$ ; exchange striction and excited-state exchange interaction (Cotton-Mouton effect). The latter is closely related to two-magnon inelastic Raman scattering. In either case, for crystals of symmetry lower than cubic, it can be shown that<sup>29</sup>

$$\frac{d(\Delta n)_m}{dT} = \sum_{\alpha} g_{\alpha} \sum_{i,j} \frac{d}{dT} \langle \vec{S}_i \cdot \vec{S}_j \rangle_{\alpha}. \quad (11)$$

Since the magnetic specific heat  $C_m$  can be expressed as

$$C_m = \sum_{\alpha} J_{\alpha} \sum_{i,j} \frac{d}{dT} \langle \vec{S}_i \cdot \vec{S}_j \rangle_{\alpha}, \quad (12)$$

it follows that  $d(\Delta n)/dT$  will be proportional to  $C_m$  only if either of the two conditions hold:

(i) each  $J_{\alpha}$  is proportional to the corresponding  $g_{\alpha}$  in exactly the same way as every other—a rather unlikely event unless, of course, only one  $J_{\alpha}$  and  $g_{\alpha}$  are of any importance, or

(ii) all of the spin-spin correlations  $\langle \vec{S}_i \cdot \vec{S}_j \rangle_{\alpha}$  have the same temperature dependence.

If all of the  $J_{\alpha}$  are short ranged (as, for example, is the case of  $\text{MnF}_2$ ), then close to the phase transition, where the correlation length becomes larger than the range of any exchange interaction, the second condition above will

be obtained. Hence for  $|t| \ll 1$ , the critical behavior of  $[d(\Delta n)/dT]_m$  and  $C_m$  should be proportional to each other and the correct critical exponents and amplitude ratios should be obtained from birefringence measurements. Indeed this has been shown to be the case for  $\text{MnF}_2$  and  $\text{FeF}_2$ .<sup>5</sup> From the analysis given above it is clear that the proportionality extends well outside the critical region for  $\text{MnF}_2$ , from which we must conclude that condition (i) is satisfied as well. This implies the dominance of the next-near-neighbor exchange interaction in this particular case.

In conclusion, we have demonstrated that for  $\text{MnF}_2$  the small lattice contribution  $[d(\Delta n)/dT]_L$  can be adequately estimated and subtracted from  $d(\Delta n)/dT$ , leaving only the magnetic part  $[d(\Delta n)/dT]_m$ . We have shown that the proportionality between  $C_m$  and  $[d(\Delta n)/dT]_m$  is not limited to the critical region but is valid over the entire temperature range  $5 \leq T \leq 100$  K, with the proportionality constant independently obtained from total entropy considerations. This demonstration gives credence to the use of  $d(\Delta n)/dT$  vs  $T$  data not only for obtaining the asymptotic behavior of  $C_m$  in the critical region but also for examining magnetic crossover behavior as  $|t|$  increases. Such an analysis of the  $\text{MnF}_2$  and  $\text{FeF}_2$  data has been performed.<sup>5</sup>

#### ACKNOWLEDGMENTS

We wish to thank P. Nordblad for the use of his specific heat data. The birefringence samples were grown by N. Nighman. This work has been supported in part by National Science Foundation Grant No. DMR-80-17582.

\*Present address: Brookhaven National Laboratory, Upton, NY 11973.

<sup>1</sup>J. F. Dillon, Jr., J. Appl. Phys. **29**, 1286 (1958); J. Magn. Magn. Mater. **31-34**, 1 (1983).

<sup>2</sup>I. R. Jahn and H. Dachs, Solid State Commun. **9**, 1617 (1971).

<sup>3</sup>I. R. Jahn, Phys. Status Solidi B **57**, 681 (1973).

<sup>4</sup>A. S. Borovik-Romanov, N. M. Kreines, and M. A. Talalaev, Pis'ma Zh. Eksp. Teor. Fiz. **13**, 80 (1971) [JETP Lett. **37**, 890 (1973)]; A. S. Borovik-Romanov, N. M. Kreines, A. A. Pankov, and M. A. Talalaev, Zh. Eksp. Teor. Fiz. **64**, 1762 (1973) [Sov. Phys.—JETP **37**, 890 (1973)].

<sup>5</sup>D. P. Belanger, P. Nordblad, A. R. King, V. Jaccarino, L. Lundgren, and O. Beckman, J. Magn. Magn. Mater. **31-34**, 1095 (1983).

<sup>6</sup>P. Nordblad, D. P. Belanger, A. R. King, V. Jaccarino, and H. J. Guggenheim, J. Magn. Magn. Mater. **31-34**, 1093 (1983).

<sup>7</sup>J. Ferré, J. Phys. C **16**, 3971 (1983).

<sup>8</sup>P. Nordblad, D. P. Belanger, A. R. King, V. Jaccarino, and H. Ikeda, Phys. Rev. B **27**, 278 (1983).

<sup>9</sup>K. Iio, M. Sakatani, and K. Nagata, J. Phys. Soc. Jpn. **45**, 1567 (1978).

<sup>10</sup>K. Iio, H. Hyodo, N. Nagata, and I. Yamada, J. Phys. Soc.

- Jpn. **44**, 1393 (1978).
- <sup>11</sup>I. R. Jahn, J. B. Merkel and H. Ott, *Solid State Commun.* **19**, 151 (1976).
- <sup>12</sup>D. P. Belanger, A. R. King, and V. Jaccarino, *J. Appl. Phys.* **53**, 2704 (1982).
- <sup>13</sup>D. P. Belanger, F. Borsa, A. R. King, and V. Jaccarino, *J. Magn. Magn. Mater.* **15-18**, 807 (1980).
- <sup>14</sup>D. P. Belanger, A. R. King, V. Jaccarino, and J. Cardy, *Phys. Rev. B* **28**, 2522 (1983).
- <sup>15</sup>I. B. Ferreira, A. R. King, V. Jaccarino, J. Cardy, and H. J. Guggenheim, *Phys. Rev. B* **28**, 5192 (1983).
- <sup>16</sup>C. G. M. Kirby, *Temperatures, Its Measurements and Control in Science and Industry*, edited by H. H. Plumb (Instrument Society of America, Pittsburgh, 1972), Vol. 4, Part 2, p. 511.
- <sup>17</sup>J. S. Browder, *J. Phys. Chem. Solids* **36**, 193 (1975).
- <sup>18</sup>A. S. Borovik-Romanov, N. M. Kreines, and J. Pačes, *Zh. Eksp. Teor. Fiz.* **77**, 2477 (1979) [*Sov. Phys.—JETP* **50**, 1198 (1979)].
- <sup>19</sup>P. Nordblad and D. P. Belanger, unpublished results.
- <sup>20</sup>R. L. Melcher, *Phys. Rev. B* **2**, 733 (1970).
- <sup>21</sup>H. M. Kandil, J. D. Greiner, A. C. Ayers, and J. F. Smith, *J. Appl. Phys.* **52**, 759 (1981).
- <sup>22</sup>W. Jauch and H. Dachs, *Solid State Commun.* **14**, 657 (1974).
- <sup>23</sup>S. S. Todd, *J. Am. Chem. Soc.* **71**, 4115 (1941).
- <sup>24</sup>K. Haefner, thesis, University of Chicago, 1964 (unpublished).
- <sup>25</sup>W. O. Boo and J. W. Stout, *J. Chem. Phys.* **65**, 3929 (1976).
- <sup>26</sup>G. S. Rushbrooke and P. J. Wood, *Mol. Phys.* **1**, 257 (1958).
- <sup>27</sup>G. Ahlers, *Rev. Mod. Phys.* **52**, 489 (1980), and references to other reviews of critical phenomena therein.
- <sup>28</sup>J. C. Le Guillou and J. Zinn-Justin, *Phys. Rev. B* **21**, 3976 (1980).
- <sup>29</sup>G. A. Gehring, *J. Phys. C* **10**, 531 (1977), and references therein.
- <sup>30</sup>G. A. Gehring, P. J. Becker, and I. R. Jahn, *Solid State Commun.* **17**, 1257 (1975).
- <sup>31</sup>C. A. Rotter, J. G. Traylor, and H. G. Smith, *Bull. Am. Phys. Soc.* **20**, 300 (1975), and Ref. 32b.
- <sup>32</sup>(a) R. Almairac, thesis, Université des Sciences et Techniques de Languedoc, Montpellier, France, 1975 (unpublished); (b) H. G. Smith and N. Wakabayashi, in *Dynamics of Solids and Liquids by Neutron Scattering*, Vol. 3 of *Topics in Current Physics*, edited by S. W. Lovesey and T. Springer (Springer, New York, 1977), p. 77.